Experimental and thermodynamic study of Co-Fe and Mn-Fe based mixed metal oxides for thermochemical energy storage application

Laurie Andre, Stéphane Abanades, Laurent Cassayre

Experimental and Thermodynamic Study of Co-Fe and Mn-Fe Based Mixed Metal Oxides for Thermochemical Energy Storage Application

Laurie André[1], Stéphane Abanades[1, a)], Laurent Cassayre[2]

[1] *Processes, Materials, and Solar Energy Laboratory, PROMES-CNRS, 7 Rue du Four Solaire, 66120 Font-Romeu, France*
[2] *Laboratoire de Génie Chimique, Université de Toulouse, CNRS, INPT, UPS, Toulouse, France*

[a)] *Corresponding author:* stephane.abanades@promes.cnrs.fr

Abstract. Metal oxides are potential materials for thermochemical heat storage, and among them, cobalt oxide and manganese oxide are attracting attention. Furthermore, studies on mixed oxides are ongoing, as the synthesis of mixed oxides could be a way to answer the drawbacks of pure metal oxides, such as slow reaction kinetics, loss-in-capacity over cycles or sintering, selected for thermochemical heat storage application. The addition of iron oxide is under investigation and the obtained results are presented. This work proposes a comparison of thermodynamic modelling with experimental data in order to identify the impact of iron oxide addition to cobalt oxide and manganese oxide. Fe addition decreased the redox activity and energy storage capacity of Co_3O_4, whereas the cycling stability of Mn_2O_3 was significantly improved with added Fe amounts above 20 mol% while the energy storage capacity was unchanged. The thermodynamic modelling method to predict the behavior of the Mn-Fe-O and Co-Fe-O systems was validated, and the possibility to identify other mixed oxides becomes conceivable, by enabling the selection of transition metals additives for metal oxides destined for thermochemical energy storage applications.

INTRODUCTION

The purpose of thermal energy storage in solar power plants is to store concentrated solar heat in the form of chemical energy during on-sun hours and then to use it during off-sun hours, thus enabling energy production according to needs. Thermal energy storage (TES) can be achieved using three main routes: latent, sensible and thermochemical heat storage [1]. This study focuses on thermochemical heat storage, which shows advantages over latent and sensible heat storage, including higher energy storage densities, possible heat storage at room temperature in the form of stable solid materials, and long term storage in a large temperature range (400-1200°C) with a constant restitution temperature. Concentrated solar power (CSP) can provide the heat source required for endothermal/exothermal reversible reactions involved in thermochemical energy storage (Eq. 1, 2) in order to store solar energy in the form of chemical bonds. When combined with CSP systems the continuous production of electricity in power plants becomes possible. The reaction enthalpy is stored in the reaction products during the heat charge (Eq. 1), and can be released by reversing the reaction during the discharge (Eq. 2).

$$MO_n + \text{Heat} \rightarrow MO_{n-1} + \tfrac{1}{2}\, O_2\,(g) \quad (1)$$

$$MO_{n-1} + \tfrac{1}{2}\, O_2\,(g) \rightarrow MO_n + \text{Heat} \quad (2)$$

Cobalt oxide, Co_3O_4, and manganese oxide, Mn_2O_3, are two of the most studied metal oxides considered as promising materials for thermochemical energy storage. Experiments showed that Co_3O_4 is the most suited raw material given the fast reaction kinetics and complete reaction reversibility [2-6]. However, the cost and potential

toxicity of cobalt oxide requires the development of other alternative materials. Optimization of materials reactivity is required for the other metal oxide species by using e.g. doping strategies, controlled synthesis techniques for tailored morphology or stabilization with inert materials to alleviate sintering effects. The effect of the morphology of the material has been studied, for instance, by Agrafiotis *et al*. (2015) [2, 3] who achieved thirty redox cycles with porous foam of Co_3O_4. Karagiannakis *et al*. (2014) [4] studied cobalt oxide, Co_3O_4/CoO, in the form of flow-through pellets and stated that these structures show better reaction kinetics than cobalt oxide as a powder, due to better heat transfer characteristics of the structured material. They also studied manganese oxide, Mn_2O_3/Mn_3O_4, in the form of flow-through pellets. The material showed better reaction kinetics than those obtained with its powder form. Because of the very slow re-oxidation kinetics of manganese oxide, the re-oxidation occurs generally in two steps, one during the cooling and the next one during the re-heating of the next cycle [4]. The addition of a secondary metal oxide can be a way to modify the properties of a pure oxide.

Improvement of materials properties and flexibility such as reaction kinetics and reaction temperature tuning can be obtained by the addition of dopants. For example, Mn_2O_3 is known for its slow re-oxidation kinetics [4], which affects its cycling stability. The doping with transition metals can relieve this issue [3, 7]. The present study aims at investigating the effect of Fe addition on the performances and thermodynamic properties of Co and Mn-based mixed metal oxides which have been identified as interesting candidates for thermochemical energy storage. The optimal mixed metal oxide composition to reach the highest performances for TES is addressed, encompassing high reaction enthalpy, stability upon cycling, low temperature gap between reduction and re-oxidation, and reaction in a temperature range adapted to CSP. The addition of transition metals is investigated as a way to answer the drawbacks of pure metal oxides, such as slow reaction kinetics [4], sintering [8] or loss-in-capacity over cycles [9]. Block *et al.* (2014) [7] reported that both addition of iron oxide to cobalt oxide or addition of cobalt oxide to iron oxide results in lower enthalpies of reaction compared to those of the pure oxides. However, they estimated that cobalt oxide doped with 10% of iron oxide possesses higher reduction/oxidation reversibility than pure cobalt oxide and still shows high enthalpy of reaction. Pagkoura *et al.* (2014) [10] showed that cobalt oxide with 10-20w% of iron oxide shows good thermo-mechanical stability over ten redox cycles. Carillo *et al*. (2014) [8] showed that the addition of iron oxide does not allow avoiding the sintering encountered with Mn_2O_3 but helps to increase the heat storage density of the material. Furthermore, the addition of iron helped to stabilize and enhance the oxidation rate of manganese oxide over an experiment of thirty redox cycles. According to their study, the fastest and most stable oxidation reaction was obtained for Mn_2O_3 doped with 20% Fe.

The possibility to predict the optimal amount of transition metal to be used and its impact on the material's properties, such as the transition temperatures, the phases formed and encountered during the heating, the structure changes and the oxygen exchange capacity, is required to assess the suitability of the redox process. For a better understanding and prediction of the behavior of Co-Fe-O and Mn-Fe-O systems at high temperatures, this work proposes a comparison of thermodynamic modelling performed with FactSage and of experimental studies for validating thermodynamic predictions.

An advantage of using metal oxides as thermochemical energy storage material is the use of air as the heat transfer fluid that can be processed in an open-loop system. For this reason, the thermodynamic modelling calculations take into account an atmosphere of P_{O_2} = 0.21 atm. The experiments are conducted in the same atmosphere, using 20%O_2/Ar as a representative gaseous mixture. The mass loss (O_2 storage capacity), the temperatures of reduction and oxidation and the enthalpies of reaction were measured and compared to calculations given by thermodynamics.

SYNTHESIS AND CHARACTERIZATION

All the powders were synthesized via a modified Pechini method, using metal nitrates, citric acid and ethylene glycol in aqueous solution [7]. The Fe molar ratio presented in percentage in the following is based on a Fe/(Fe+Co) and Fe/(Fe+Mn) mole ratio. The powders were all calcined at 750°C for 4h in air in order to fully eliminate the organic fraction and residues of the synthesis, and to stabilize the structure. The complete removal of organics was confirmed by the absence of extra mass loss during the first heating step of thermogravimetric analyses. Higher calcination temperatures were not considered to avoid the reduction of the materials during the synthesis. The powders were characterized by X-ray diffraction (XRD) before being studied in redox cycles. XRD analysis was

performed (Fig. 1) at room temperature using a PANalytical XPert Pro diffractometer (CuKα radiation, λ = 0.15418 nm). X-ray diffraction measurements of θ-θ symmetrical scans were made over an angular range of 10 to 80°. The step size and the time per step were fixed at 0.01° and 20 s respectively. The contribution from $AlK\alpha_2$ was removed and the X-ray diffractograms were recorded and studied using the PANalytical software. The instrumental function was determined using a reference material (SRM 660, lanthanum hexaboride, LaB6 polycrystalline sample) and can be expressed by a polynomial function [11]. Pure Co_3O_4 and Mn_2O_3, and Co_3O_4 and Mn_2O_3 with iron incorporated into the structure, were synthesized. The more the iron added to Co_3O_4, the more amorphous the material gets (Fig. 1.b). For both Co_3O_4 and Mn_2O_3, the peaks for iron oxide are covered by noise or by the base-oxide peaks, and are only detected for the material containing the largest amount of iron. The synthesized oxide phases were corresponding to the structures of (i) a cubic spinel solution $(Co_{1-x}Fe_x)_3O_4$ (Fig. 1a and b) and (ii) a bixbyite solution $(Mn_{1-x}Fe_x)_2O_3$ [12] (Fig. 1c and d). Traces of iron oxide (Fe_3O_4 and Fe_2O_3, respectively) were detected for the samples with the highest Fe content (Fig. 1b and d).

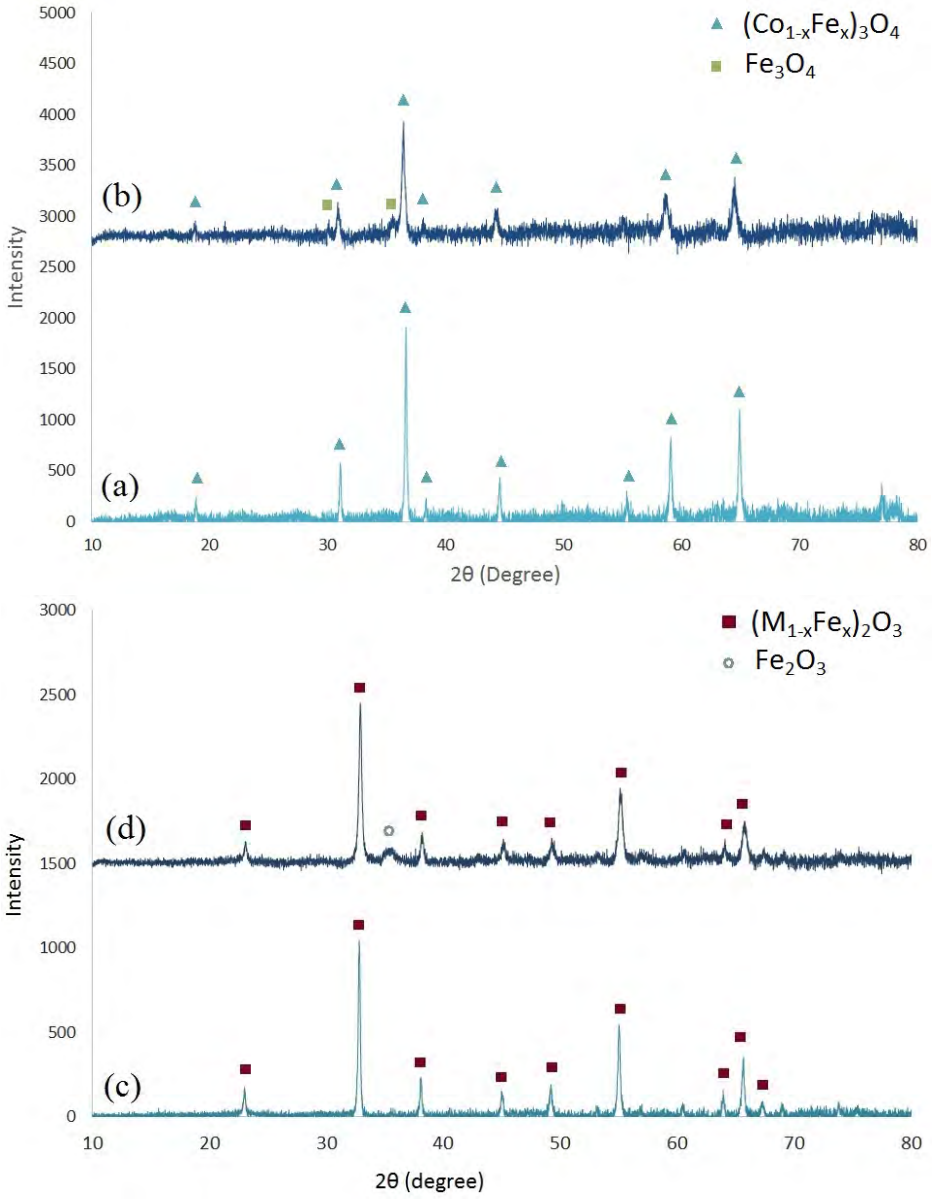

FIGURE 1. XRD analysis of (a) Co_3O_4 with 5 mol% Fe, (b) Co_3O_4 with 25 mol% Fe, (c) Mn_2O_3 with 10 mol% Fe and (d) Mn_2O_3 with 50 mol% Fe.

EXPERIMENTAL RESULTS

Experimental data concerning transition temperatures during redox process, oxygen storage capacity of redox materials and reaction enthalpies were obtained by using simultaneous thermogravimetric analysis (TGA) and differential scanning calorimetry (DSC), using a Netzsch STA 449 F3 System. Reduction-oxidation cycles were performed in a 20%O_2/Ar atmosphere, between 800°C and 1050°C, with pure cobalt oxide and cobalt oxide mixed with 5 mol%, 10 mol% and 25 mol% Fe (Fig. 3), and between 750°C and 1050°C with pure Mn_2O_3 and manganese oxide mixed with 10, 20, 30, 40 and 50 mol% Fe. Each TGA profile also contains a separate reduction step under Ar, in order to get information about the reduction temperature of the material under inert atmosphere. The heating rate was 20 °C/min for the reduction step, and the cooling rate was 10°C/min for the re-oxidation step. The gas flow rates used were 10 Nml/min for O_2 and 40 Nml/min for Ar. About 50 mg of powder was placed into an alumina crucible and then analyzed in TGA coupled with DSC. A series of three cycles was performed for each studied formulation as it proves sufficient in order to determine their suitability for achieving reversible reactions and to assess a possible chemical deactivation of the materials as a result of a loss of redox stability during thermal treatment.

Experimental data were compared with equilibrium calculations in order to validate the thermodynamic modelling approach. The FactSage software was combined with the FToxid database, which includes a full description of the thermochemical properties of the oxide phases in the Fe-Mn-O and Fe-Co-O systems, in order to calculate the behavior of mixed oxides intended for thermochemical energy storage applications. The theoretical mass loss, Δm, was calculated at atmospheric pressure and under air between 800°C and 1050°C, and the enthalpy of phase transition was determined.

Cobalt Oxide

Cobalt oxide is considered as a promising thermochemical energy storage material due to its high gravimetric storage density and high cycling stability when compared with other metal oxide candidates. The reduction temperature of Co_3O_4 to CoO in air atmosphere was measured between 880 and 930°C [4, 6, 10, 13].

A section of the Co-Fe-O phase diagram, presented in Fig. 2a, has been calculated for P_{O_2} = 0.21 atm. The phase diagram shows that the iron content greatly influences the composition and the amount of the monoxide phase formed when heating the spinel phase. As an example, Fig. 2b presents the influence of the temperature on the conversion rate for cobalt oxide mixed with 20 mol% Fe: a temperature of about 1380°C is required to fully convert the spinel phase into the monoxide phase.

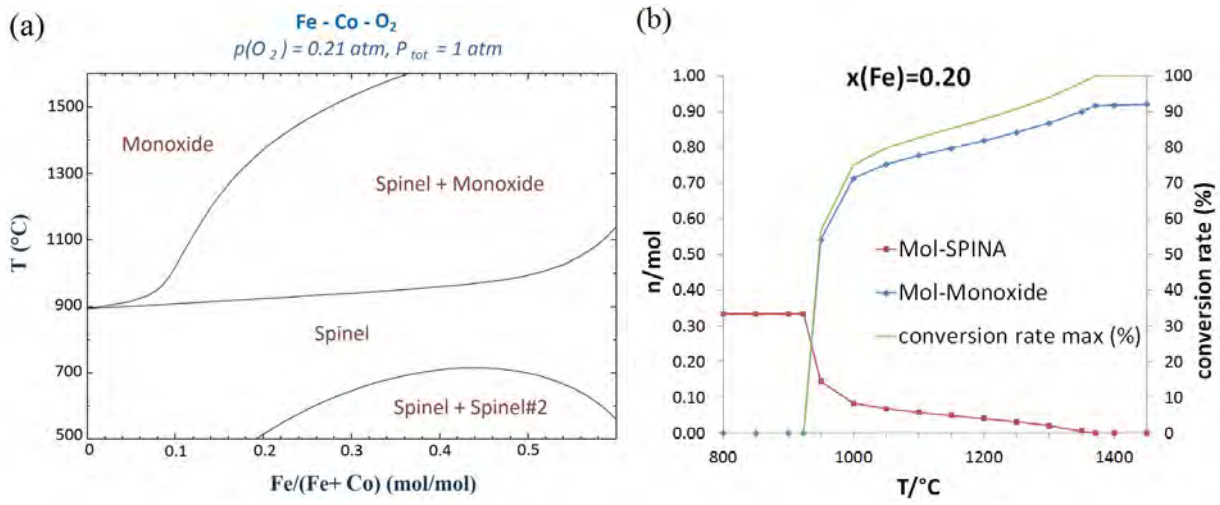

FIGURE 2. (a) Co-Fe-O phase diagram under air, (b) example of phase composition and conversion rate evolution with the temperature for Co_3O_4 with addition of 20 mol% Fe.

The TGA of Co_3O_4 shows the variations in the amount of O_2 exchanged, Δm, for Co_3O_4 with addition of various amounts of iron (Fig. 3). Co_3O_4 containing the highest amount of iron (Fig. 3a) shows the lowest reduction extent

(the mass loss, Δm, during heating up to 1050°C is the lowest). Increasing the amount of iron in the material thus reduces the mass of O_2 it is able to release. As observed in the phase diagram (Fig. 2a), the material composition transitions from a spinel phase to a spinel plus monoxide phase when heating above ~900-1000°C for Fe content in the range considered in this study (5-25%). The higher the iron amount added to the material, the lower the reduction to cobalt monoxide and the lower the amount of O_2 released by the material. In thermochemical energy storage, the enthalpy of the reaction is related to the oxygen storage capacity of the material. When the redox activity of the material is lowered, there is a decrease of reaction enthalpy. Thus, with more iron added, the gravimetric energy storage density is decreased compared with pure Co_3O_4, resulting in less storage capacity per gram of material. The theoretical estimations of Δm obtained from thermodynamics show a linear decrease with increasing Fe content and are perfectly in agreement with the obtained experimental values (Fig. 4a). However, the cycling stability of cobalt oxide suffers from the addition of iron oxide, as the re-oxidation conversion rate is slightly decreasing over multiple cycles for Co-Fe mixed oxides, which is not the case for pure Co_3O_4 (Fig. 4a.). In Fig. 4a are represented, along with calculated values, the maximum values of Δm measured for each composition, which means the highest amount of O_2 released during reduction, and the average Δm for the three redox cycles. For pure Co_3O_4, the average Δm remains the same as the theoretical value and the maximum value measured experimentally. This means that the O_2 released and regained did not change, confirming the material cycling stability. For the samples containing iron, since the average Δm falls below the theoretical and maximum value, a slight loss in O_2 exchange capacity upon cycling is evidenced (Fig. 4a).

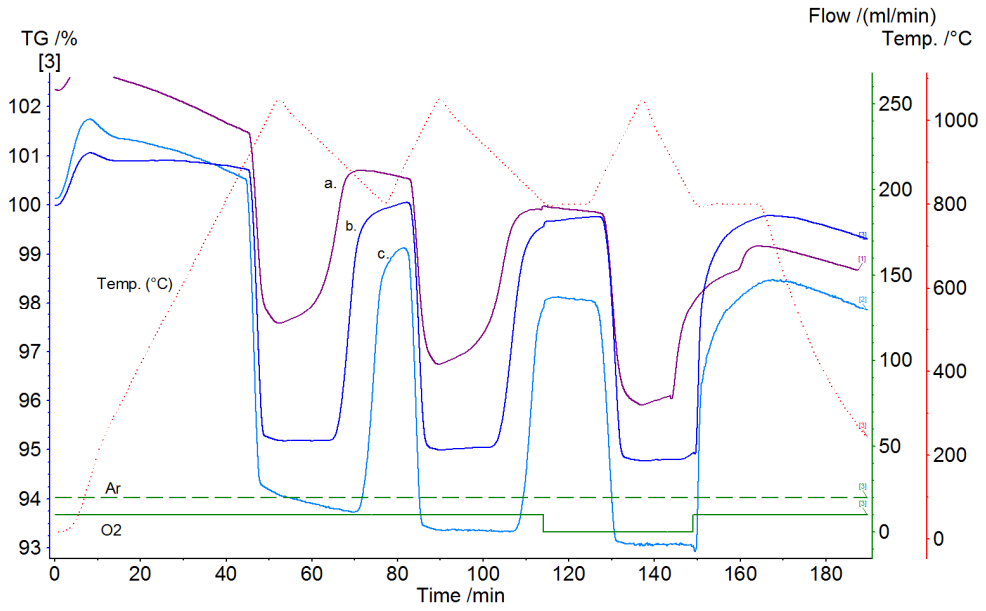

FIGURE 3. TG analysis of Co_3O_4/CoO + (a) 25 mol% Fe, (b) 10 mol% Fe, (c) 5 mol% Fe

The influence of the incorporation of iron oxide on reaction temperatures was also studied and temperatures at peak reaction rate, i.e. the temperatures at which the reaction kinetics reached its maximum, were measured. A gradual increase of the reduction and oxidation temperatures is observed with increasing amount of iron in the material (Fig. 4b). An effect of Fe addition on the temperature gap between reduction and oxidation is also visible. As both temperatures rise with more Fe addition, it can be noticed that, at 25 mol% of added Fe, the gap between the reduction and oxidation temperatures has been reduced (Fig. 4b). The reduction of this gap in temperature is interesting for large-scale application since it reduces the amount of energy spent for the heating and cooling of the system. The measured enthalpies of reaction are decreasing with increasing amount of Fe added, which agrees with the decrease in Δm. The highest enthalpy measured is 471.6 kJ/kg for pure Co_3O_4, and the lowest is 194.4 kJ/kg for Co_3O_4 with 25 mol% Fe, which correlates well with the observed Δm differences in the TGA measurements of the two formulations (Fig. 4a); while, for pure Co_3O_4, the theoretical enthalpy is about 844 kJ/kg according to thermodynamics [14], and about 747 kJ/kg according to FactSage models. The noteworthy discrepancy between the measured and theoretical enthalpies is the result of Co_3O_4 structural changes attributed to spin-state change [14]. A

similar decrease in enthalpy with increasing Fe content was observed by Block et al (2016) [7] as they measured an enthalpy of 433 kJ/kg for Co_3O_4 with 13 mol% Fe, and a lower enthalpy of 165 kJ/kg for Co_3O_4 with 33 mol% Fe.

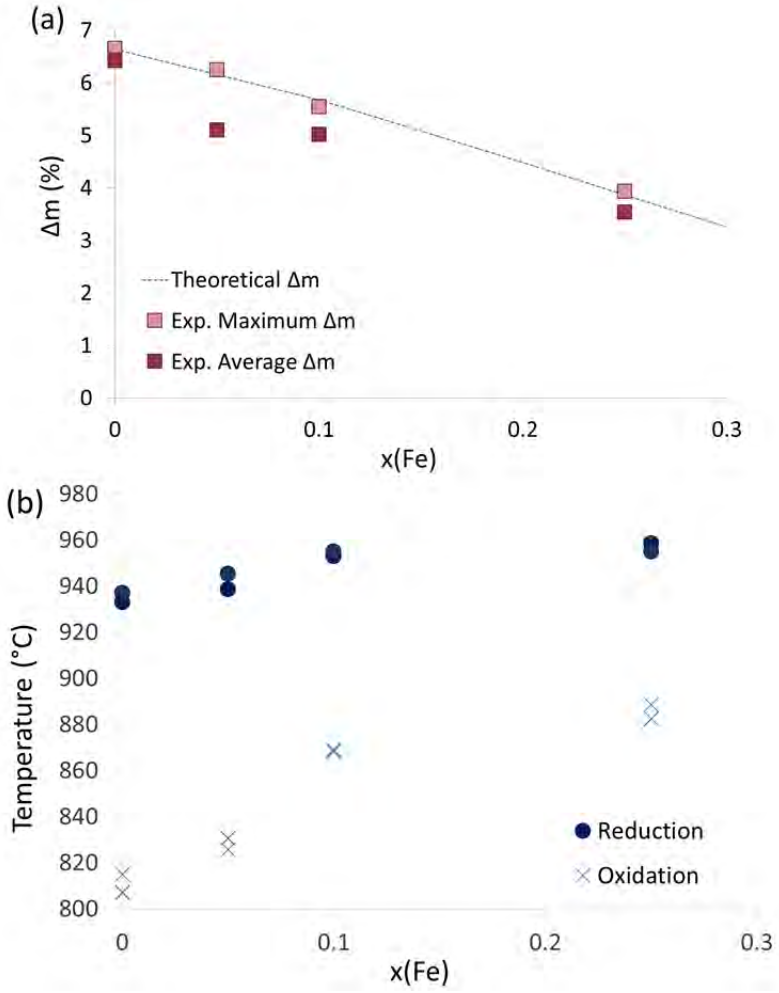

FIGURE 4. (a) Average and maximal experimental Δm (%) compared to theoretical Δm between 800°C and 1050°C (under atmosphere condition of 20% O_2), (b) Experimental temperatures at peak reaction rate for pure cobalt oxide and mixed Co-Fe oxides.

The Co_3O_4/CoO redox pair shows very good cycling stability, however, the addition of iron is shown to slightly affect it. According to the phase diagram of the Co-Fe-O system, the addition of iron to Co_3O_4 results in a lower amount of O_2 exchanged, due to an incomplete conversion of the spinel phase at 1050°C. The addition of iron to Co_3O_4 also increases the reduction and oxidation temperatures, while decreasing the gap in temperature between the reduction and the oxidation step with more iron added.

Manganese Oxide

The Mn_2O_3/Mn_3O_4 couple was studied by TGA coupled with DSC with and without addition of iron. The reduction step of Mn_2O_3 was observed in the range of 920-1000°C and the notably slow re-oxidation was observed in the range of 850-500°C with a gravimetric energy storage density of 110 kJ/kg. The re-oxidation happens in two steps, the first one being during the cooling and in between 700°C-500°C and the second one being during the re-heating and in the range of 500-850°C [10]. The temperature of the TGA program used here is ranging between 750°C and 1050°C. The calculated Mn-Fe-O phase diagram is presented in Fig. 5, for P_{O_2} = 0.21 atm. It can be

observed that, when heated under air, manganese oxides mixed with less than 20% of iron go through two consecutive two-phase zones before reaching full reduction into a single spinel phase. In contrast, above about 20 mol% Fe, the material fully transforms from the bixbyite Mn_2O_3 phase to the cubic spinel Mn_3O_4. Thus the amount of O_2 exchanged, Δm, remains the same whatever the amount of iron, until reaching 50 mol% (limit studied here) (Fig. 5a). This is well illustrated with the example of the phase transition of Mn_2O_3 with 20 mol% Fe in Fig. 5b. The phase transition is fast during heating and takes place promptly in a very narrow range of temperature, at about 960°C, according to experimental results.

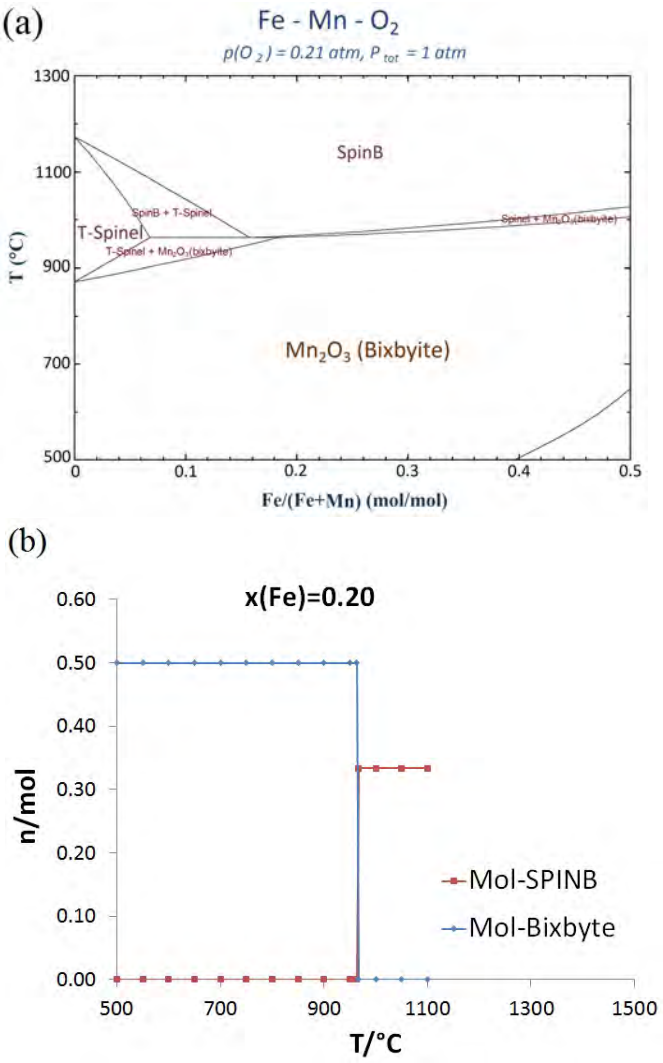

FIGURE 5. (a) Mn-Fe-O phase diagram under air, (b) example of phase composition evolution with the temperature for Mn_2O_3 with addition of 20 mol% Fe.

TGA shows that the sample with the composition going through the two-phase zones, (i.e. containing 10 mol% Fe added to Mn_2O_3), is unable to regain its full mass during oxidation, as the Δm lost during the first reduction step cannot be recovered during the re-oxidation step. Inversely, the other compositions, from 20 mol% Fe to 50 mol% Fe, are capable of regaining their lost O_2 mass in a complete reversible way. They all share the same Δm, as predicted by the Mn-Fe-O phase diagram. In addition, the measured enthalpy of reaction is in agreement with theoretical estimations, for pure Mn_2O_3, of 190.1 kJ/kg [15], and about 207.78 kJ/kg according to FactSage calculations. An average of 185.2 kJ/kg is measured for the samples with compositions between 20 mol% Fe and 50 mol% Fe. The samples of pure Mn_2O_3 and with 10 mol% Fe show similar enthalpy, 145 kJ/kg and 144.2 kJ/kg

respectively, measured for the first reduction step with full conversion. The highest enthalpy of 193.3 kJ/kg is measured for Mn_2O_3 with 20 mol% Fe. Experimental and theoretical mass variations, Δm, were compared. It is observed that Δm remains stable with the addition of iron to manganese oxide, in agreement with the phase diagram. This tendency is consistent with the experimental results, showing that the maximal values of Δm are similar to the theoretical ones.

Mn_2O_3 shows cycling stability issues due to sintering. This phenomenon is reflected by the average experimental Δm, showing a decrease of redox activity during cycling. Mn_2O_3 mixed with 10 mol% Fe also loses cycling stability, regaining only 31% of its lost mass. However, from 20 mol%Fe to 50 mol% Fe added, a great improvement is observed, since the average Δm value remains close to the maximum Δm value and to the theoretical value (Fig. 6a.). The addition of iron to Mn_2O_3 reduces the sintering of the material and enhances the cycling stability, as already observed previously [8].

As for the influence of Fe incorporation in Mn_2O_3 on the reaction temperatures, a similar tendency as with cobalt oxide is obtained. The reduction and oxidation temperatures of Mn_2O_3 increase with increasing amount of added iron (Fig. 6b). The addition of iron oxide to Mn_2O_3 enhances its cycling stability (in the range 20-50 mol% Fe) and also changes its reaction temperature. This way, the reaction temperature can be tuned. In addition to an increase of the temperature, further addition of iron also reduces the gap in temperature between the reduction and the oxidation step.

In summary, this study showed that the addition of iron to manganese oxide reduces the sintering of Mn_2O_3 and enhances the cycling stability of the material. Also, the higher the amount of iron added to Mn_2O_3, the higher the reaction temperatures. In addition, the gap in temperature between the reduction and the oxidation decreases with higher iron content.

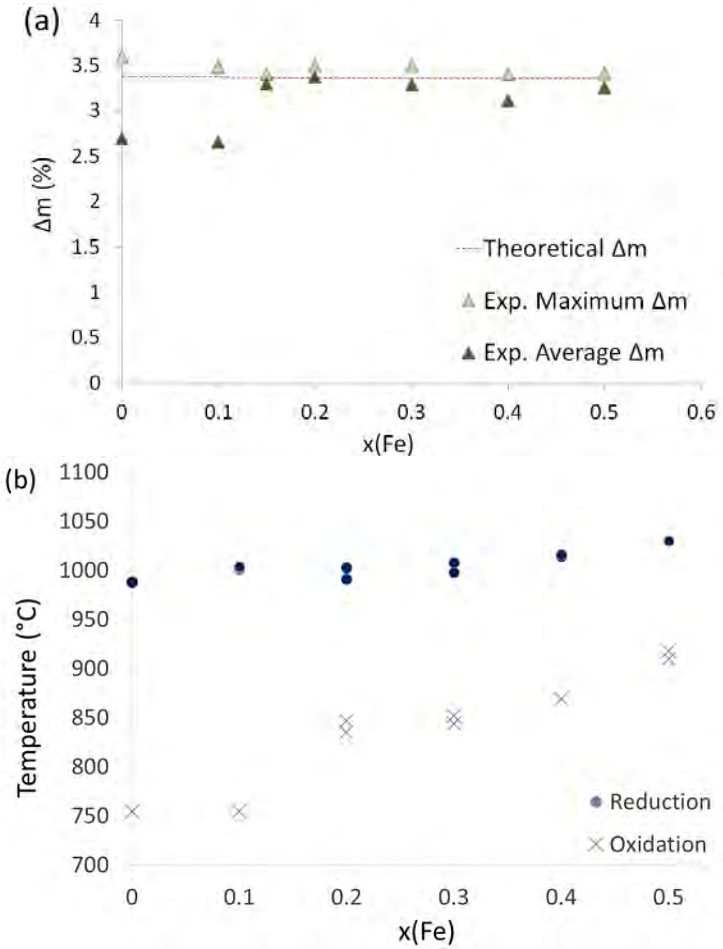

FIGURE 6. (a) Average and maximal experimental Δm (%) compared to theoretical Δm (under atmosphere condition of 20% O_2), (b) Experimental temperatures at peak reaction rate for pure manganese oxide and mixed Mn-Fe oxides.

CONCLUSION

The effect of Fe addition in Co and Mn-based oxides was studied experimentally and results were compared with thermodynamic calculations. The addition of iron to Mn_2O_3 is promising since it can be used to tune the temperature of redox reactions, to reduce the gap in temperature hysteresis between the reduction and the oxidation step, as well as to enhance the re-oxidation kinetics and cycling stability of the material by countering the sintering issue of Mn_2O_3. Conversely, the incorporation of iron to Co_3O_4 has negative effect on the redox performances since the maximum amount of O_2 exchanged is lowered when the amount of iron added is increased. The increasing amount of iron added to Co_3O_4 reduces the maximum oxygen mass exchanged during a redox cycle. The addition of iron to Co and Mn-based oxides also results in an increase of the reaction temperatures, while slightly lowering the gap in temperature between the reduction and oxidation step. The comparison of the obtained experimental data with FactSage thermodynamic modelling proves that this method is effective for predicting the behavior of mixed oxides since it results in consistent phase transition temperatures and reliable oxygen storage capacities. It could be further used for selecting other transition metals to enhance the properties of mixed metal oxides for thermochemical energy storage application.

REFERENCES

1. A. H. Abedin and M. A. Rosen, The open renewable energy journal **4**, 42-46 (2011).
2. C. Agrafiotis, M. Roeb, M. Schücker and C. Sattler, Solar Energy **114**, 440–458 (2015).
3. C. Agrafiotis, S. Tescari, M. Roeb, M. Schücker and C. Sattler, Solar Energy **114**, 459-475 (2015).
4. G. Karagiannakis, C. Pagkoura, A. Zygogianni, S. Lorentzou and A. G. Konstadopoulos, Energy Procedia **49**, 820-829 (2014).
5. M. Neises, S. Tescari, L. De Oliveira, M. Roeb, C. Sattler and B. Wong, Solar Energy **86**, 3040–3048 (2012).
6. S. Tescari, C. Agrafiotis, S. Breuer, L. De Oliveira, M. Neises, M. Roeb and C. Sattler, Energy Procedia **49**, 1034–1043 (2014).
7. T. Block, N. Knoblauch and M. Shmücker, Thermochemica Acta **577**, 25-32 (2014).
8. A. J. Carillo, D. P. Serrano, P. Pizzaro and J. M. Coronado, Chem Sus Chem **8**, 1947-1954 (2015).
9. A. J. Carillo, D. P. Serrano, P. Pizzaro and J. M. Coronado, J Mater Chem A **2**, 19435-19443 (2014).
10. C. Pagkoura, G. Karagiannakis, A. Zygogianni, S. Lorentzou, M. Kostoglou, A. G. Konstandopoulos and M. Rattenburry, Solar Energy **108**, 146-163 (2014).
11. E. Beche, G. Peraudeau, V. Flaud and D. Perarnau, Surface and Interface Analysis **44,** 1045-1050 (2012).
12. Lai J-i, Shafi KVPM, Ulman A, Yang N-L, Cui M-H, Vogt T, Estournès C. Mixed iron-manganese oxide nanoparticles. Chem. Soc. Div. Fuel Chem., **48(2)** (2003) 729-730.
13. B. Ehrhart, E. Coker, N. Siegel, A. Weimer, Energy Procedia **49**, 762-771 (2014).
14. T. Block, M Schmucker, Solar Energy **126**, 195–207 (2016).
15. L. André, S. Abanades, G. Flamant, Renewable & Sustainable Energy Reviews **64**, 703-715 (2016).